





RAPID COMMUNICATION | APRIL 08 2024

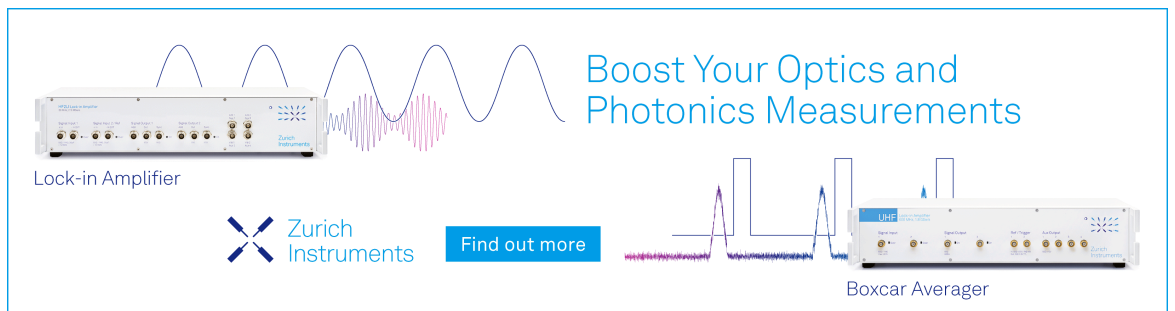
Transition metals of Pt and Pd on the surface of topological insulator Bi_2Se_3

Lina Liu  ; Ireneusz Miotkowski; Dmitry Zemlyanov ; Yong P. Chen 




J. Chem. Phys. 160, 141101 (2024)

<https://doi.org/10.1063/5.0191941>



Boost Your Optics and
Photonics Measurements

Lock-in Amplifier

 Zurich
Instruments

[Find out more](#)

Boxcar Averager

Transition metals of Pt and Pd on the surface of topological insulator Bi_2Se_3

Cite as: *J. Chem. Phys.* **160**, 141101 (2024); doi: [10.1063/5.0191941](https://doi.org/10.1063/5.0191941)

Submitted: 17 December 2023 • Accepted: 22 March 2024 •

Published Online: 8 April 2024



View Online



Export Citation



CrossMark

Lina Liu,^{1,2,3,a)}  Ireneusz Miotkowski,¹ Dmitry Zemlyanov,³  and Yong P. Chen^{1,2,3,4,a)}

AFFILIATIONS

¹Department of Physics and Astronomy, Purdue University, West Lafayette, Indiana 47907, USA

²Institute of Physics and Astronomy and Villum Center for Hybrid Quantum Materials and Devices, Aarhus University, 8000 Aarhus-C, Denmark

³Birck Nanotechnology Center, Purdue University, West Lafayette, Indiana 47907, USA

⁴Purdue Quantum Science and Engineering Institute and School of Electrical and Computer Engineering, Purdue University, West Lafayette, Indiana 47907, USA

^{a)}Authors to whom correspondence should be addressed: lnliu@phys.au.dk and yongchen@purdue.edu

ABSTRACT

Transition metal catalysts supported on topological insulators are predicted to show improved catalytic properties due to the presence of topological surface states, which may float up to the catalysts and provide robust electron transfer. However, experimental studies of surface structures and corresponding catalytic properties of transition metal/topological insulator heterostructures have not been demonstrated so far. Here, we report the structures, chemical states, and adsorption behaviors of two conventional transition metal catalysts, Pt and Pd, on the surface of Bi_2Se_3 , a common topological insulator material. We reveal that Pt forms nanoparticles on the Bi_2Se_3 surface. Moreover, the interaction between Pt and surface Se is observed. Furthermore, thermal dosing of O_2 onto the Pt/ Bi_2Se_3 heterostructure leads to no oxygen adsorption. Detailed scanning tunneling microscopy study indicates that Pt transforms into PtSe_2 after the thermal process, thus preventing O_2 from adsorption. For another transition metal Pd, it exhibits approximate layer-island growth on Bi_2Se_3 , and Pd–Se interaction is also observed. Our work provides significant insights into the behaviors of transition metals on top of a common topological insulator material and will assist in the future design of catalysts built with topological materials.

© 2024 Author(s). All article content, except where otherwise noted, is licensed under a Creative Commons Attribution (CC BY) license (<https://creativecommons.org/licenses/by/4.0/>). <https://doi.org/10.1063/5.0191941>

INTRODUCTION

In the past decade, topological materials have been extensively studied due to their topologically protected surface states and their fascinating electronic properties, giving rise to a variety of potential applications in electronics, spintronics, and energy storage and conversion.^{1–3} The low-dissipation electron transport in topological surface states (TSSs) provides stable and fast charge transfer channels for catalytic reactions, offering new possibilities for designing highly efficient catalysts, as well as promising new catalytic mechanisms.^{4,5} A number of recent experiments have unveiled outstanding catalytic performance in different topological materials. For instance, Weyl semimetals are presented to be good catalysts for both hydrogen and oxygen evolution reactions.^{6–8} Pt-based topological semimetals not only exhibit hydrogen evolution performance

close to that of commercial Pt/C but also possess a low Pt mass ratio, thus lowering the catalyst cost.^{9,10} Very recently, topological insulator Bi_2Se_3 has been shown to be an efficient catalyst for oxidative carbonylation of amines with a high yield of 99% even at room temperature, much lower than the temperatures required for most noble metal catalysts.¹¹

Topological materials can also boost catalysis when served as supporting substrates for traditional catalysts since it has been suggested that TSSs may float to the overlayer and influence the electronic structures of catalysts.¹² As a result, enhancement of CO and O_2 adsorption has been theoretically predicted on gold-covered Bi_2Se_3 , and facilitation of CO oxidation by TSSs was predicted.¹³ Similarly, single-layer $\text{ZnSe}/\text{Bi}_2\text{Se}_3$ heterostructure has been predicted to exhibit optimal hydrogen adsorption energy, leading to promising catalytic performance for hydrogen evolution reaction

(HER).¹⁴ Furthermore, Xiao *et al.* have pointed out that TSSs have dual effects.¹⁵ The HER catalytic ability of different transition metal catalysts may be enhanced or suppressed, depending on the initial adsorption strength between metals and hydrogen. However, compared with a fair amount of theoretical research, the experimental progress of catalysts supported on topological materials remains very limited. Surface structures and catalytic properties of transition metals on topological material substrates have not been determined so far, greatly hindering the study of catalytic properties of conventional catalysts influenced by topological effects.

Here, we study the structures of transition metals on the surface of topological insulator Bi_2Se_3 and the interaction between them by various microscopic and spectroscopic techniques. The topographic and atomic structures of deposited Pt on Bi_2Se_3 were imaged by scanning tunneling microscopy (STM). Chemical states of Pt on Bi_2Se_3 were characterized by x-ray photoemission spectroscopy (XPS), and charge interaction between them was evaluated by high-resolution electron energy loss spectroscopy (HREELS). Oxygen (O_2) adsorption was tested on the Pt/ Bi_2Se_3 heterostructure by introducing O_2 in ultrahigh vacuum (UHV), and structures and chemical states after O_2 dosing were studied. In addition, topographic structures of deposited Pd on Bi_2Se_3 were discussed. Our work discloses the surface structures and properties of transition metals on a topological insulator material and may provide insights into catalyst design based on quantum materials in the future.

RESULTS AND DISCUSSION

Bi_2Se_3 consists of quintuple layers with intralayer Se–Bi–Se–Bi–Se atomic sequences and weak interlayer van der Waals (vdW) interactions, which ensures easy cleavage between layers and obtaining a clean surface. Bi_2Se_3 single crystal was cleaved in a UHV environment with a base pressure of $\sim 5 \times 10^{-9}$ mbar in this study. After cleavage, the sample was directly transferred to the STM chamber for characterization without breaking UHV. Figure 1(a) demonstrates a clean Bi_2Se_3 surface with a step height of 9.7 Å, corresponding to the step height of a quintuple layer.¹⁶ The atomic resolution STM image [inset in Fig. 1(a)] illustrates the hexagonal atomic lattice with a periodicity of 4.1 Å, consistent with Se-termination on the surface.¹⁶ We conducted Pt deposition

at room temperature on Bi_2Se_3 using a Pt e-beam evaporator installed on the UHV chamber. After deposition, Pt nanoparticles were observed randomly and nearly homogeneously distributed on the surface [Fig. 1(b)]. Apparent heights of the Pt nanoparticles distribute in the range from 2.8 to 7.3 Å with most particles demonstrating a height of ~ 4.4 Å [Fig. 1(c)]. The evolution of surface morphologies after different Pt deposition times suggests that Pt may undergo the Volmer–Weber growth (island growth) mode on Bi_2Se_3 , similar to the growth of Au on Bi_2Se_3 ¹⁷ (see details in the supplementary material, Fig. S1). When Pt is deposited, due to lack of surface diffusion (Fig. S2) and possible reactions between Pt and Se,^{18,19} Pt atoms and clusters may bond to the substrate immediately. This results in the growth of random Pt nanoparticles on the Bi_2Se_3 surface. In addition, we also note that the lattice mismatch between Pt and Bi_2Se_3 is large, $\sim 33\%$. This could be another reason that leads to the island growth.

To understand the interaction between Pt and Bi_2Se_3 , XPS evaluation of the chemical states of Pt and Se was carried out. As shown in Fig. 2(a), Pt core levels demonstrate binding energies at 71.8 and 75.1 eV, corresponding to the Pt $4f_{7/2}$ and $4f_{5/2}$ orbitals, respectively. These binding energies are ~ 0.6 eV higher than those of metal Pt (71.2 and 74.5 eV),²⁰ indicating the apparent loss of electrons of the deposited Pt. Meanwhile, two sets of peaks appear in the Se 3d spectra [Fig. 2(b)]. The major set exhibits binding energies at 53.4 and 54.3 eV, corresponding to Se $3d_{5/2}$ and $3d_{3/2}$ orbitals in Bi_2Se_3 , respectively²¹ [inset in Fig. 2(b)]. The minor set of binding energies takes place at 54.2 and 55.0 eV, which are ~ 1.4 eV lower than the binding energies of elemental Se.²⁰ Combined with the higher binding energies of Pt, it indicates Pt demonstrates strong interaction with surface Se after deposition.²² The XPS peaks of the minor set of Se can be attributed to the Pt–Se interaction.

HREELS was employed to further explore the charge interaction between Pt and Bi_2Se_3 by measuring the collective modes of Bi_2Se_3 . In the energy loss spectrum of the as-cleaved Bi_2Se_3 [Fig. 2(c)], a sharp peak at 21.7 meV and a broad peak at 74 meV were observed, corresponding to the characteristic optical phonon mode and bulk plasmon mode of Bi_2Se_3 , respectively.²³ Note that Bi_2Se_3 is typically n-type doped with a substantial amount of carriers in the bulk. After Pt deposition, an energy shift of the bulk plasmon mode was clearly observed, resulting in the new plasmon excitation

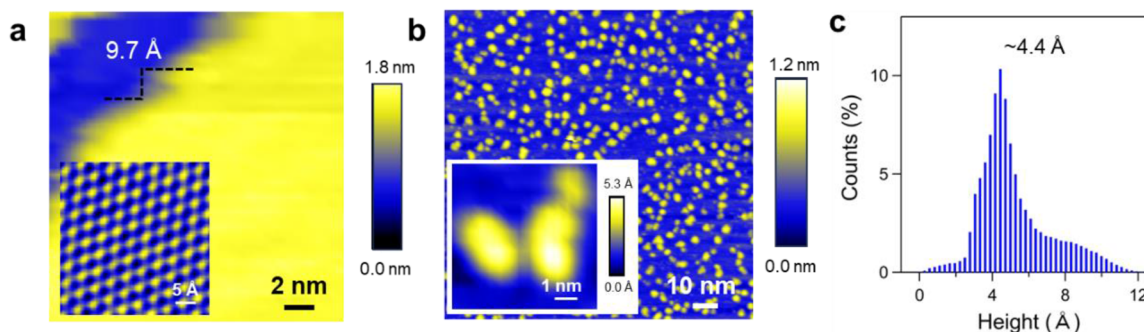


FIG. 1. Bi_2Se_3 and Pt deposition. (a) An STM topographic image of the surface of as-cleaved Bi_2Se_3 . Inset: an atomic resolution STM image of the as-cleaved Bi_2Se_3 surface. $V_b = 1.3$ V and $I_t = 1.0$ nA. (b) An STM topographic image of the surface of as-cleaved Bi_2Se_3 after Pt deposition for 7 min. $V_b = -1.0$ V and $I_t = 1.0$ nA. Inset: a zoomed-in STM image of a few Pt nanoparticles. (c) Height distribution of the deposited Pt nanoparticles.

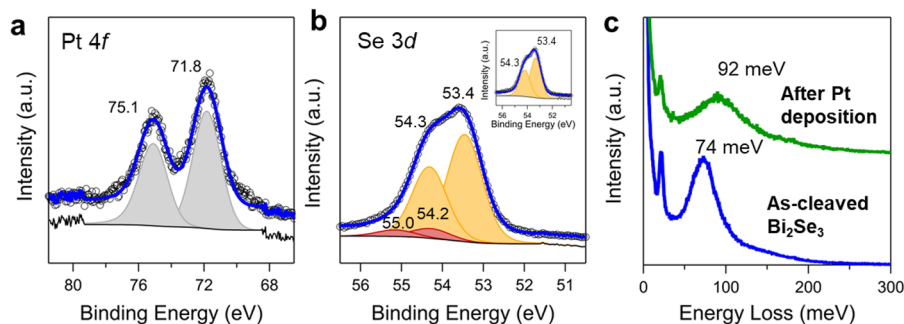


FIG. 2. Spectroscopic measurements before and after Pt deposition on Bi_2Se_3 . [(a) and (b)] Pt 4f and Se 3d XPS spectra after Pt deposition on Bi_2Se_3 , respectively. Inset in (b) shows Se 3d XPS spectra of the as-cleaved Bi_2Se_3 . (c) HREELS spectra of the as-cleaved Bi_2Se_3 and after Pt deposition.

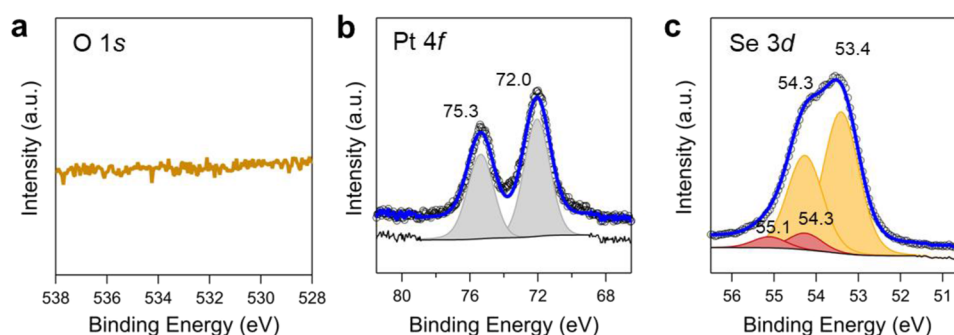


FIG. 3. XPS spectra after thermal dosing of O_2 . [(a)–(c)] O 1s, Pt 4f, and Se 3d XPS spectra after thermal dosing of O_2 to the Pt/ Bi_2Se_3 heterostructure, respectively.

at a higher energy of 92 meV. This energy shift can be attributed to increased carrier density (at least in the region near the surface as probed by HREELS) in Bi_2Se_3 ,²⁴ indicating strong electron doping from the deposited Pt. Moreover, the low-energy peak at 21.7 meV, which corresponds to the A_{1g} phonon mode of Bi_2Se_3 , was shifted to 21.2 meV after Pt deposition (Fig. S3), possibly resulting from combined effects of lattice constant change at the Bi_2Se_3 surface and electron–phonon coupling.

As an enhancement of O_2 adsorption was predicted on Bi_2Se_3 supported transition metals,^{13,15} we introduced O_2 into the UHV chamber to examine the oxygen adsorption properties of the Pt/ Bi_2Se_3 heterostructure. To ensure a reasonable amount of dosing, we applied thermal dosing of O_2 with a pressure at $\sim 5 \times 10^{-6}$ mbar, which is in between high and low pressures for O_2 adsorption on Pt according to a previous study.²⁵ After dosing at 250 °C for 10 min, XPS did not show oxygen traces in the O 1s spectrum [Fig. 3(a)]. Moreover, binding energies of Pt 4f peaks appear at 72.0 and 75.3 eV [Fig. 3(b)], shifted to higher energies by 0.2 eV compared with those of Pt just after deposition [Fig. 2(a)]. The major set of Se binding energies (from Bi_2Se_3) remains at 53.4 and 54.3 eV. The minor set of Se displays binding energies at 54.3 and 55.1 eV [Fig. 3(c)], 0.1 eV higher than those after Pt deposition [Fig. 2(b)] and close to the binding energies of PtSe_2 .²⁶ The binding energies' shift of both Pt and Se indicates that it is changed toward PtSe_2 after the thermal process during the dosing. Thus, it is highly possible that the

binding sites of Pt are fully occupied by Se, resulting in no active sites for O_2 adsorption.

To better understand the Pt/ Bi_2Se_3 heterostructure after thermal dosing of O_2 , we conducted STM to image the topographic and atomic structures. Interestingly, instead of randomly distributed nanoparticles, Pt appears as orientated two-dimensional (2D) triangular islands on the surface [Fig. 4(a)]. Some of the islands are more

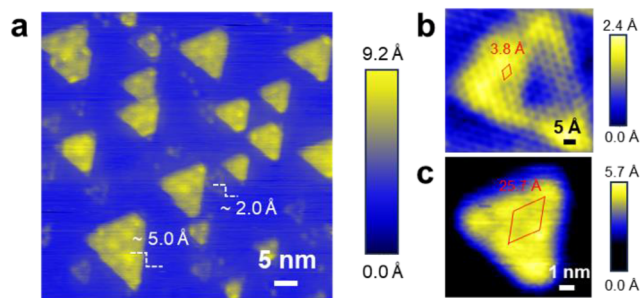


FIG. 4. STM images of Pt after thermal dosing of O_2 . (a) A topographic STM image of Pt after the thermal process. [(b) and (c)] Atomic resolution and zoomed-in STM images of two triangular islands with typical heights of ~ 2.0 and ~ 5.0 Å, respectively. $V_b = -1.0$ V and $I_t = 1.0$ nA.

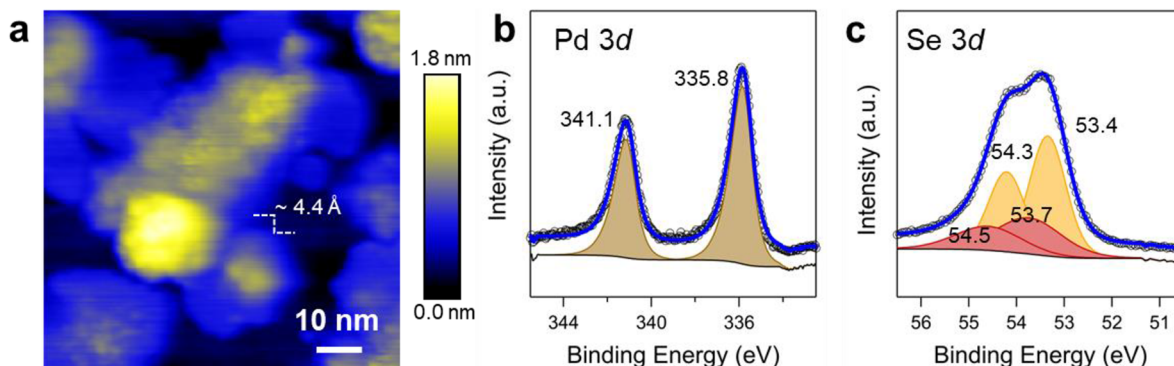


FIG. 5. Deposition of Pd on the surface of Bi_2Se_3 . (a) An STM topographic image of the deposited Pd on Bi_2Se_3 . $V_b = -1.3$ V and $I_t = 1.0$ nA. [(b) and (c)] Pd 3d and Se 3d XPS spectra after deposition.

pronounced with bigger heights of ~ 5.0 Å, which is consistent with the height of monolayer PtSe_2 .²⁷ While some other islands appear to have the central parts more immersed in Bi_2Se_3 , leaving noticeable triangular edges with a smaller height of ~ 2.0 Å on the surface. This phenomenon suggests that Pt undergoes interdiffusion into Bi_2Se_3 . Atomic scale STM images were carried out to resolve the atomic structures. Figure 4(b) shows the atomic arrangements of a lower island and the hexagonal lattices illustrate the periodicity of 3.8 Å, close to the lattice constant of PtSe_2 of 3.75 Å.²⁷ The zoomed-in STM image of a higher island displays a moiré pattern (periodicity of 25.7 Å) [Fig. 4(c)], which suggests a 2D stacking between the triangular island and substrate. We also conducted a parallel experiment in which we heated the Pt/ Bi_2Se_3 heterostructure in UHV (same heating condition with that of O_2 thermal dosing but without O_2). We observed that the surface demonstrates similar triangular islands (Fig. S4) with those in Fig. 4(a) after heating. This suggests that it is the heating that makes the transformation of Pt nanoparticles to PtSe_2 islands.

In addition to Pt, we also studied another well-known transition metal catalyst, Pd, on the surface of Bi_2Se_3 . Rather than nanoparticles, the deposited Pd exhibits random shape 2D islands with a typical height of ~ 4.4 Å on the surface [Fig. 5(a)]. On the 2D islands, three-dimensional (3D) growth of bulky clusters was observed. This indicates an approximate Stranski–Krastanov layer-plus-island growth mode^{28,29} of Pd on Bi_2Se_3 . The different growth modes of Pt and Pd on Bi_2Se_3 may result from different degrees of interaction between the transition metals and Bi_2Se_3 (see details in Fig. S5). Similar to Pt, XPS spectra of Pd show ~ 0.6 eV higher binding energies (335.8 and 341.1 eV) [Fig. 5(b)] than those of metal Pd,²⁰ indicating the Pd–Se interaction. Two sets of binding energies were again observed in the Se 3d spectra [Fig. 5(c)]: the set at lower binding energies corresponds to Bi_2Se_3 , and the set at the higher binding energies of 53.7 and 54.5 eV is related to Pd–Se interaction on the surface.

The common interaction feature of Pt and Pd with Bi_2Se_3 is consistent with the results of previous studies, which reported the interfacial interaction between Bi_2Se_3 and a series of contact metals^{17,30} (Au, Ir, Pd, etc.). Given that this hinders the adsorption capability of transition metals as we observed in the O_2 adsorption test for Pt on Bi_2Se_3 , depositing a relatively thicker layer of

transition metal may help screen the properties of interfacial interaction and, thus, unveil intrinsic adsorption properties of transition metals. In the meantime, the evolution of TSSs and their effectiveness as a function of the thickness of the deposited layer could be traced in future studies, although TSSs are reported to be relatively robust to surface doping at low impurity concentration.³¹

CONCLUSIONS

In summary, we demonstrated the structures and chemical states of transition metal Pt and Pd on the surface of topological insulator Bi_2Se_3 . Pt exhibited randomly distributed nanoparticles and significant interaction with surface Se after deposition. Thermal dosing of O_2 did not result in any oxygen adsorption on Pt, which can be attributed to the complete occupation of Pt binding sites by Se. Atomic resolution STM images suggested the transformation of Pt to PtSe_2 after the thermal process. In contrast to Pt nanoparticles, Pd demonstrated an approximate 2D–3D layer-island growth mode on the Bi_2Se_3 surface. Pd also demonstrated apparent interaction with surface Se after deposition. Our work shed light on the interaction between traditional transition metal catalysts and a common topological insulator material and will guide the rational design of future topological catalysts.

SUPPLEMENTARY MATERIAL

Experimental details of single crystal growth and cleavage, deposition, O_2 dosing and characterizations, and additional experimental results can be found in the supplementary material.

ACKNOWLEDGMENTS

This work was supported in part by the U.S. Department of Energy (Office of Basic Energy Sciences) (Award No. DE-SC0019215), Multidisciplinary University Research Initiatives (MURI) Program (Award No. FA9550-20-1-0322) (experimental), and the Villum Investigator Program (Grant No. 25931) (analysis).

AUTHOR DECLARATIONS

Conflict of Interest

The authors have no conflicts to disclose.

Author Contributions

Lina Liu: Conceptualization (lead); Data curation (lead); Formal analysis (lead); Writing – original draft (lead); Writing – review & editing (equal). **Ireneusz Miotkowski:** Resources (equal); Writing – review & editing (equal). **Dmitry Zemlyanov:** Conceptualization (equal); Data curation (equal); Formal analysis (equal); Resources (equal); Writing – review & editing (equal). **Yong P. Chen:** Conceptualization (equal); Funding acquisition (lead); Supervision (lead); Writing – review & editing (lead).

DATA AVAILABILITY

The data that support the findings of this study are available from the corresponding authors upon reasonable request.

REFERENCES

- P. Z. Liu, J. R. Williams, and J. J. Cha, “Topological nanomaterials,” *Nat. Rev. Mater.* **4**, 479 (2019).
- H. X. Luo, P. F. Yu, G. W. Li, and K. Yan, “Topological quantum materials for energy conversion and storage,” *Nat. Rev. Phys.* **4**, 611 (2022).
- N. Kumar, S. N. Guin, K. Manna, C. Shekhar, and C. Felser, “Topological quantum materials: From the viewpoint of chemistry,” *Chem. Rev.* **121**, 2780 (2021).
- G. W. Li and C. Felser, “Heterogeneous catalysis at the surface of topological materials,” *Appl. Phys. Lett.* **116**, 070501 (2020).
- R. K. Xie, T. Zhang, H. M. Weng, and G. L. Chai, “Progress, advantages, and challenges of topological material catalysts,” *Small Sci.* **2**, 2100106 (2022).
- C. R. Rajamathi, U. Gupta, N. Kumar, H. Yang, Y. Sun, V. Süß, C. Shekhar, M. Schmidt, H. Blumtritt, P. Werner, B. Yan, S. Parkin, C. Felser, and C. N. R. Rao, “Weyl semimetals as hydrogen evolution catalysts,” *Adv. Mater.* **29**, 1606202 (2017).
- G. Li, Q. Xu, W. Shi, C. Fu, L. Jiao, M. E. Kamminga, M. Yu, H. Tuysuz, N. Kumar, V. Süß, R. Saha, A. K. Srivastava, S. Wirth, G. Auffermann, J. Gooth, S. Parkin, Y. Sun, E. Liu, and C. Felser, “Surface states in bulk single crystal of topological semimetal $\text{Co}_3\text{Sn}_2\text{S}_2$ toward water oxidation,” *Sci. Adv.* **5**, eaaw9867 (2019).
- D. Shao, J. Deng, H. Sheng, R. Zhang, H. Weng, Z. Fang, X. Q. Chen, Y. Sun, and Z. Wang, “Large spin hall conductivity and excellent hydrogen evolution reaction activity in unconventional $\text{PtTe}_{1.75}$ monolayer,” *Research* **6**, 0042 (2023).
- Q. Yang, G. Li, K. Manna, F. Fan, C. Felser, and Y. Sun, “Topological engineering of Pt-group-metal-based chiral crystals toward high-efficiency hydrogen evolution catalysts,” *Adv. Mater.* **32**, e1908518 (2020).
- G. Li, C. Fu, W. Shi, L. Jiao, J. Wu, Q. Yang, R. Saha, M. E. Kamminga, A. K. Srivastava, E. Liu, A. N. Yazdani, N. Kumar, J. Zhang, G. R. Blake, X. Liu, M. Fahlman, S. Wirth, G. Auffermann, J. Gooth, S. Parkin, V. Madhavan, X. Feng, Y. Sun, and C. Felser, “Dirac nodal arc semimetal PtSn_4 : An ideal platform for understanding surface properties and catalysis for hydrogen evolution,” *Angew. Chem., Int. Ed.* **58**, 13107 (2019).
- J. Li, J. Wu, S. W. Park, M. Sasase, T. N. Ye, Y. Lu, M. Miyazaki, T. Yokoyama, T. Tada, M. Kitano, and H. Hosono, “Topological insulator as an efficient catalyst for oxidative carbonylation of amines,” *Sci. Adv.* **9**, eadh9104 (2023).
- Q. L. He, Y. H. Lai, Y. Lu, K. T. Law, and I. K. Sou, “Surface reactivity enhancement on a $\text{Pd}/\text{Bi}_2\text{Te}_3$ heterostructure through robust topological surface states,” *Sci. Rep.* **3**, 2497 (2013).
- H. Chen, W. Zhu, D. Xiao, and Z. Zhang, “CO oxidation facilitated by robust surface states on Au-covered topological insulators,” *Phys. Rev. Lett.* **107**, 056804 (2011).
- L. Q. Li, J. Zeng, W. Qin, P. Cui, and Z. Y. Zhang, “Tuning the hydrogen activation reactivity on topological insulator heterostructures,” *Nano Energy* **58**, 40 (2019).
- J. P. Xiao, L. Z. Kou, C. Y. Yam, T. Frauenheim, and B. H. Yan, “Toward rational design of catalysts supported on a topological insulator substrate,” *ACS Catal.* **5**, 7063 (2015).
- C. L. Song, Y. L. Wang, Y. P. Jiang, Y. Zhang, C. Z. Chang, L. L. Wang, K. He, X. Chen, J. F. Jia, Y. Y. Wang, Z. Fang, X. Dai, X. C. Xie, X. L. Qi, S. C. Zhang, Q. K. Xue, and X. C. Ma, “Topological insulator Bi_2Se_3 thin films grown on double-layer graphene by molecular beam epitaxy,” *Appl. Phys. Lett.* **97**, 143118 (2010).
- M. Fanetti, I. Mikulska, K. Ferfolja, P. Moras, P. M. Sheverdyeva, M. Panighel, A. Lodi-Rizzini, I. Piš, S. Nappini, M. Valant, and S. Gardonio, “Growth, morphology and stability of Au in contact with the Bi_2Se_3 (0 0 0 1) surface,” *Appl. Surf. Sci.* **471**, 753 (2019).
- T. Y. Su, H. Medina, Y. Z. Chen, S. W. Wang, S. S. Lee, Y. C. Shih, C. W. Chen, H. C. Kuo, F. C. Chuang, and Y. L. Chueh, “Phase-engineered PtSe_2 -layered films by a plasma-assisted selenization process toward all PtSe_2 -based field effect transistor to highly sensitive, flexible, and wide-spectrum photoresponse photodetectors,” *Small* **14**, e1800032 (2018).
- Y. Wang, L. Li, W. Yao, S. Song, J. T. Sun, J. Pan, X. Ren, C. Li, E. Okunishi, Y. Q. Wang, E. Wang, Y. Shao, Y. Y. Zhang, H. T. Yang, E. F. Schwier, H. Iwasawa, K. Shimada, M. Taniguchi, Z. Cheng, S. Zhou, S. Du, S. J. Pennycook, S. T. Pantelides, and H. J. Gao, “Monolayer PtSe_2 , a new semiconducting transition-metal-dichalcogenide, epitaxially grown by direct selenization of Pt,” *Nano Lett.* **15**, 4013 (2015).
- J. F. Moulder, W. F. Stickle, P. E. Sobol, and K. D. Bomben, *Handbook of X-Ray Photoelectron Spectroscopy* (Perkin-Elmer Corporation, Physical Electronics Division, Eden Prairie, Minnesota, USA, 1992).
- K. Ferfolja, M. Fanetti, S. Gardonio, M. Panighel, I. Piš, S. Nappini, and M. Valant, “A cryogenic solid-state reaction at the interface between Ti and the Bi_2Se_3 topological insulator,” *J. Mater. Chem. C* **8**, 11492 (2020).
- C. D. Spataro and F. Léonard, “Fermi-level pinning, charge transfer, and relaxation of spin-momentum locking at metal contacts to topological insulators,” *Phys. Rev. B* **90**, 085115 (2014).
- X. Jia, S. Zhang, R. Sankar, F. C. Chou, W. Wang, K. Kempa, E. W. Plummer, J. Zhang, X. Zhu, and J. Guo, “Anomalous acoustic plasmon mode from topologically protected states,” *Phys. Rev. Lett.* **119**, 136805 (2017).
- A. Kogar, S. Vig, A. Thaler, M. H. Wong, Y. Xiao, D. Reig-i-Plessis, G. Y. Cho, T. Valla, Z. Pan, J. Schneeloch, R. Zhong, G. D. Gu, T. L. Hughes, G. J. MacDougall, T. C. Chiang, and P. Abbamonte, “Surface collective modes in the topological insulators Bi_2Se_3 and $\text{Bi}_{0.5}\text{Sb}_{1.5}\text{Te}_{3-x}\text{Se}_x$,” *Phys. Rev. Lett.* **115**, 257402 (2015).
- G. N. Derry and P. N. Ross, “High coverage states of oxygen adsorbed on $\text{Pt}(100)$ and $\text{Pt}(111)$ surfaces,” *Surf. Sci.* **140**, 165 (1984).
- M. Sojková, E. Dobročka, P. Hutár, V. Tašková, L. Pribusová Slušná, R. Stoklas, I. Piš, F. Bondino, F. Munnik, and M. Hulman, “High carrier mobility epitaxially aligned PtSe_2 films grown by one-zone selenization,” *Appl. Surf. Sci.* **538**, 147936 (2021).
- L. Zhang, T. Yang, M. F. Sahdan, Arramel, W. S. Xu, K. J. Xing, Y. P. Feng, W. J. Zhang, Z. Wang, and A. T. S. Wee, “Precise layer-dependent electronic structure of MBE-grown PtSe_2 ,” *Adv. Electron. Mater.* **7**, 2100559 (2021).
- N. Stranski and L. Krastanow, “Zur theorie der orientierten ausscheidung von ionenkristallen aufeinander,” *Monatsh. Chem. Verw. Teile Anderer Wiss.* **71**, 351 (1937).
- J. E. Prieto and I. Markov, “Stranski–Krastanov mechanism of growth and the effect of misfit sign on quantum dots nucleation,” *Surf. Sci.* **664**, 172 (2017).
- L. A. Walsh, C. M. Smyth, A. T. Barton, Q. X. Wang, Z. F. Che, R. Y. Yue, J. Kim, M. J. Kim, R. M. Wallace, and C. L. Hinkle, “Interface chemistry of contact metals and ferromagnets on the topological insulator Bi_2Se_3 ,” *J. Phys. Chem. C* **121**, 23551 (2017).
- T. Valla, Z. H. Pan, D. Gardner, Y. S. Lee, and S. Chu, “Photoemission spectroscopy of magnetic and nonmagnetic impurities on the surface of the Bi_2Se_3 topological insulator,” *Phys. Rev. Lett.* **108**, 117601 (2012).